Communications in Physics, Vol. 30, No. 2 (2020), pp. 171-180
DOI:10.15625/0868-3166/30/2/14814

FULL $\mathcal{O}(\alpha)$ ELECTROWEAK RADIATIVE CORRECTIONS TO $e^-e^+ \to W^-W^+$ WITH INITIAL BEAM POLARIZATION EFFECTS

PHAN HONG KHIEM[1,2,†], NGUYEN ANH THU[1,2], AND NGUYEN HUU NGHIA[1,2]

[1]*University of Science Ho Chi Minh City,* 227 *Nguyen Van Cu, District* 5*, HCM City, Vietnam*
[2]*Vietnam National University Ho Chi Minh City, Linh Trung Ward, Thu Duc District, Ho Chi Minh City, Vietnam*

[†]*E-mail:* phkhiem@hcmus.edu.vn

Received 8 Feburary 2020
Accepted for publication 21 March 2020
Published 25 April 2020

Abstract. *We calculate full $\mathcal{O}(\alpha)$ electroweak radiative corrections and $\mathcal{O}(\alpha^3)$ initial state radiation (ISR) corrections to $e^-e^+ \to W^-W^+$ with initial beam polarization effects. In phenomenological results, we study the impact of electroweak and ISR corrections on cross sections as well as their relevant distributions. We find that the corrections are order of* 10% *contributions. They are sizable contributions and should be taken into account at future lepton colliders.*

Keywords: Higher-order computations, electroweak radiative corrections, W-pair production at lepton colliders, QED corrections, numerical methods for Quantum Field Theory..

Classification numbers: 12.15.Lk, 31.30.jg.

I. INTRODUCTION

The W-pair production plays an important role at future lepton colliders. Because the most precise direct determination of the mass of W-boson (M_W) can be extracted from the production cross sections. It is emphasized that M_W is one of the most important parameters in the Standard Model (SM). The precise measurement of M_W plays a key role in updating of the global the SM fit. From the kinematic fit, we can verify SM at high energies and probe for new physics. Furthermore, we can search for the coupling of triplet gauge bosons from the corrected cross sections of this process. Last but not least, we can test the coupling of Higgs boson to W-pair. As a matter of the above facts, we can confirm the structure of non-Abelian gauge theories [1].

The evaluations for higher-order corrections to the W-pair production are necessary. Until recently, there have been available many computations for one-loop electroweak radiative corrections to the process $e^-e^+ \to W^-W^+$ at lepton colliders [2–7]. At future lepton colliders, the initial polarized beams are designed for enhancing the signal cross sections while suppressing SM backgrounds. These help to increase the measurement accuracy for probing new physics. Thus, higher-order quantum corrections to the W-pair production with the effects of the initial beam polarizations are great of interests. Especially, we calculate full $\mathcal{O}(\alpha)$ electroweak radiative corrections $e^-e^+ \to W^+W^-$ with considering the initial beam polarization effects in this article. In order to estimate the weak corrections, we also evaluate three-loop initial state radiation corrections by following the QED structure functions approach in [8, 9]. In physical results, we study the impact of electroweak, ISR corrections on cross sections as well as their relevant distributions.

This report is organized as follows. In Sec. II, we present the calculation in detail. The GRACE-Loop program is described briefly first as a tool using in this computation. After generating the matrix elements for this process, the numerical checks for the calculation is also performed in this section. We next present the structure function method which is used for simulating the ISR corrections to this reaction. The physical predictions for $e^-e^+ \to W^-W^+$ will be shown in Sec.'III. Conclusions and future prospects will be devoted in Sec. IV.

II. CALCULATIONS

Detailed calculations for the process $e^-e^+ \to W^-W^+$ in the SM are shown in this section. GRACE-Loop program [10], a generic program for the automatic calculation of scattering processes in High Energy Physics, is used for this computation. In this program, non-linear gauge fixing terms have been implemented into the Lagrangian. These terms [10] are written as follows:

$$\begin{aligned}\mathscr{L}_{GF} &= -\frac{1}{\xi_W}|(\partial_\mu - ie\tilde{\alpha}A_\mu - igc_W\tilde{\beta}Z_\mu)W^{\mu+} + \xi_W\frac{g}{2}(v+\tilde{\delta}H+i\tilde{\kappa}\chi_3)\chi^+|^2 \\ &\quad -\frac{1}{2\xi_Z}(\partial_\mu Z^\mu + \xi_Z\frac{g}{2c_W}(v+\tilde{\varepsilon}H)\chi_3)^2 - \frac{1}{2\xi_A}(\partial_\mu A^\mu)^2, \end{aligned} \tag{1}$$

where $\tilde{\alpha},\tilde{\beta},\tilde{\delta},\tilde{\varepsilon},\tilde{\kappa}$ are non-linear gauge fixing parameters. $\chi^\pm,\chi_3$ are the Nambu-Goldstone bosons. One-loop renormalization has been carried out following the Kyoto scheme [11, 12] with on-shell conditions in GRACE-Loop. For more detail of describing GRACE at one-loop, we refer Ref. [10] in which many of $2 \to 2,3$-processes have been computed successfully.

With the above non-linear gauge fixing terms, the full set of Feynman diagrams for $e^-e^+ \to W^-W^+$ process consists of 4 tree diagrams and 334 one-loop diagrams (including counter-terms

diagrams). In Fig. 1, we show some selected diagrams. The corrected cross section at full one-loop

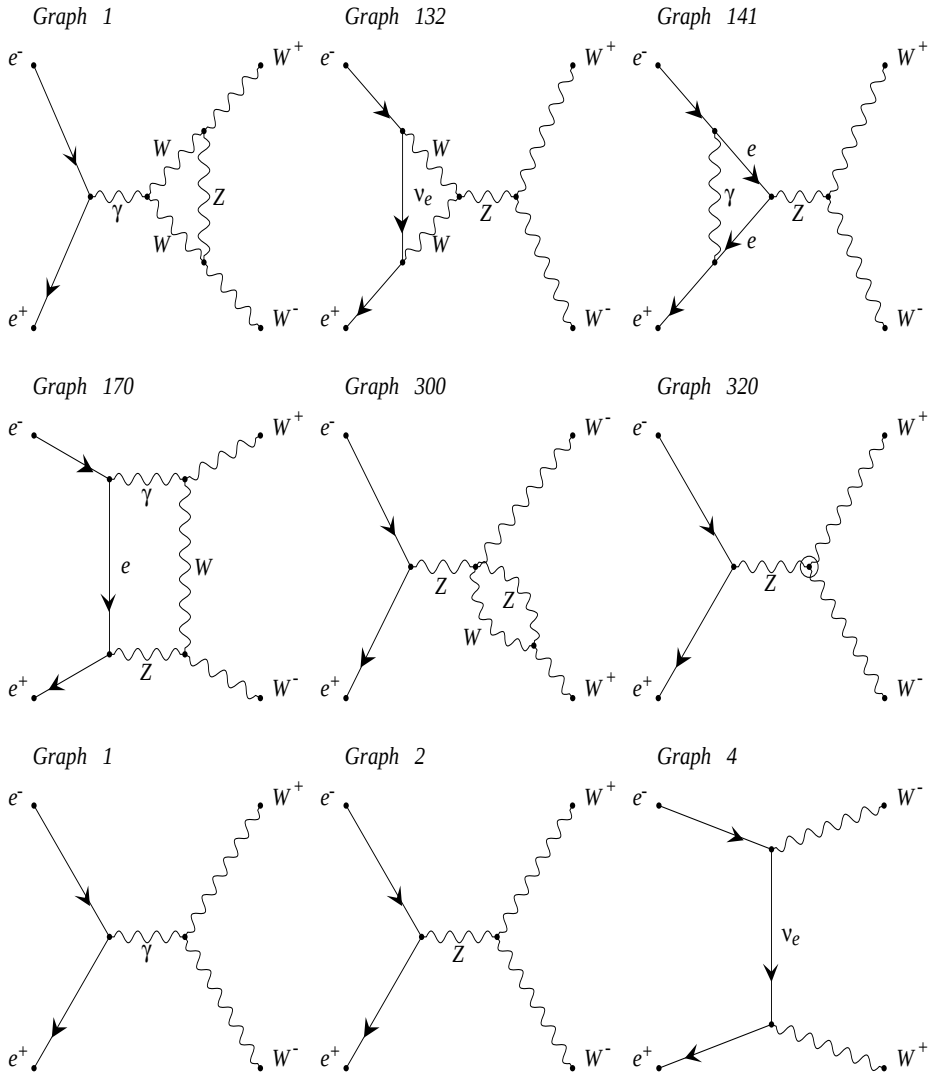

Fig. 1. Typical Feynman diagrams for the process $e^-e^+ \to W^-W^+$.

electroweak radiative corrections is computed by including the tree and one-loop virtual corrections graphs as well as the soft and hard bremsstrahlung contributions. In general, the corrected

cross section is given:

$$\sigma^{e^-e^+\to W^-W^+}_{\mathcal{O}(\alpha)} = \int d\sigma^{e^-e^+\to W^-W^+}_{\rm T} + \int d\sigma^{e^-e^+\to W^-W^+}_{\rm V}(C_{UV},\{\tilde{\alpha},\tilde{\beta},\tilde{\delta},\tilde{\epsilon},\tilde{\kappa}\},\lambda) + \int d\sigma^{e^-e^+\to W^-W^+}_{\rm T}\delta_{\rm soft}(\lambda \le E_{\gamma_S} < k_c) + \int d\sigma^{W^-W^+\gamma_H}_{\rm H}(E_{\gamma_H} \ge k_c), \quad (2)$$

where $\sigma^{e^-e^+\to W^-W^+}_{\rm T}$ presents for the tree-level cross section and $\sigma^{e^-e^+\to W^-W^+}_{\rm V}$ shows for one-loop virtual cross section which is computed from the interference between one-loop (including counter terms diagrams) and tree Feynman diagrams. As a result of the renormalized theory, this term must be independent of the ultra-violet cutoff parameter (C_{UV}). Following gauge invariance conditions, the one-loop cross section are free of the nonlinear gauge parameters. In order to regularize the IR divergences, we provide virtual photon a fictitious mass (λ). As a matter of this fact, $\sigma^{e^-e^+\to W^-W^+}_{\rm V}$ depends on the photon mass λ. This dependence then will be canceled out by taking the soft-photon contribution which is the third term in right hand side of Eq. (2), where the soft-photon factor can be found in Ref [10]. The contribution of the hard photon bremsstrahlung is the process $e^+e^- \to W^-W^+\gamma_H$ with adding an hard bremsstrahlung photon. The final results is then independent of the soft-photon cutoff energy k_c.

After generating `FORTRAN` codes for this process, we are going to perform numerical checks for the computations. In Tables 2, 3 and 4, the numerical checks for the UV finiteness, gauge invariance, and the IR finiteness at a random point in phase space are shown. The test is performed in double precision. We find that the numerical results are stable over a range of 9 digits. The k_c stability of the results are shown in Table 5. We vary k_c from 10^{-5} GeV to 10^{-2} GeV and find that the results are consistent to an accuracy better than 0.002% (seen Appendix for all Tables of data).

Furthermore, in Table 1 we cross check this work with Ref. [4] for unpolarized beams using the input parameters as in [4]. We show the tree-level cross section (upper line) and full electroweak corrections (lower line) in percentage. The results in our work are in good agreement with Ref. [4].

Table 1. Cross check this work with Ref. [4].

$\sqrt{s}$ [GeV]	This work	Ref. [4]
190	17.862(7) [pb]	17.863 [pb]
	−9.48(8)%	−9.49%
500	6.599(5) [pb]	6.599 [pb]
	−12.79(2)%	−12.74%
1000	2.464(9) [pb]	2.465 [pb]
	−15.39(6)%	−15.38%

II.1. POLARIZATION BEAMS

In GRACE program, the polarized degrees for electron and positron have been implemented by using projection operators [13] as follows:

$$\sum_{s=1,2} u_{e^-}(p)\bar{u}_{e^-}(p) = \frac{1+\lambda_{e^-}\gamma_5}{2}(\not{p}+m), \tag{3}$$

$$\sum_{s=1,2} v_{e^+}(p)\bar{v}_{e^+}(p) = \frac{1-\lambda_{e^+}\gamma_5}{2}(\not{p}-m). \tag{4}$$

Where $\lambda_{e^-} = \pm 1 (\lambda_{e^+} = \pm 1)$ are to L,R for electron (and positron). The GRACE-Loop is used to generate the following processes:

$$e_L^- e_R^+ (e_R^- e_L^+) \to W^-W^+, \tag{5}$$

$$e_L^- e_L^+ (e_R^- e_R^+) \to W^-W^+. \tag{6}$$

Having the cross sections $\sigma_{LR}, \sigma_{RL}, \sigma_{LL}$ and σ_{RR} for this reaction, we then evaluate the cross section at general polarization (P_{e^-}, P_{e^+}) for electron and positron. It is given [14]:

$$\begin{aligned}\sigma(P_{e^-}, P_{e^+}) = & \frac{1+P_{e^-}}{2}\frac{1+P_{e^+}}{2}\sigma_{RR} + \frac{1-P_{e^-}}{2}\frac{1-P_{e^+}}{2}\sigma_{LL} \\ & + \frac{1-P_{e^-}}{2}\frac{1+P_{e^+}}{2}\sigma_{LR} + \frac{1+P_{e^-}}{2}\frac{1-P_{e^+}}{2}\sigma_{RL}.\end{aligned} \tag{7}$$

For many options at future colliders, the specified values for (P_{e^-}, P_{e^+}) are not discussed in this article. For providing general results, we will only present the numerical results for the cases of $(P_{e^-}, P_{e^+}) = (\pm 1, \pm 1)$ in next section.

II.2. STRUCTURE FUNCTION METHOD

For modeling the initial-state photon radiation corrections, we follow the factorization theorems which ISR cross sections for W-pair production are expressed as a convolution of the two structure functions (SF) for two beams and of the lowest-order cross section. It is given as follows:

$$\sigma_{\rm ISR}^{e^-e^+\to W^-W^+}(s) = \int dx_1 dx_2 D(x_1, Q^2) D(x_2, Q^2) \hat{\sigma}_{\rm T}^{e^-e^+\to W^-W^+}(x_1 x_2 s), \tag{8}$$

where $D(x, Q^2)$ is the non-singlet collinear Structure Function for modeling the initial-state photon radiation at the energy scale Q^2. It presents for the probability for an electron with momentum fraction x at the energy scale Q^2 inside a electron parent. Since the emitted photons connect to all possible positions along initial fermion lines (initial beams of electron and positron). Therefore, these Feynman diagrams also obey gauge invariance. In Eq. (8), $\hat{\sigma}_{\rm T}^{e^-e^+\to W^-W^+}(x_1 x_2 s)$ is tree-level cross section for the process $e^-e^+ \to W^+W^-$ computed at the reduced center-of-mass energy $\hat{s} = x_1 x_2 s$. This tree-level cross section also obeys gauge invariance and it is generated by tree version of GRACE [10].

The factorized SF given up to third order finite terms can be found in [8,9] whose formulas are expressed as follows:

$$D(x, Q^2) = D_{GL}(x, Q^2) \sum_{i=1}^{3} d_F^{(i)} \tag{9}$$

with

$$D_{GL}(x,Q^2) = \frac{\exp\left[\frac{1}{2}\beta\left(\frac{3}{4}-\gamma_E\right)\right]}{\Gamma\left(1+\frac{1}{2}\beta\right)}\frac{1}{2}\beta\,(1-x)^{\frac{1}{2}\beta-1}, \quad (10)$$

$$d_F^{(1)}(x,Q^2) = \frac{1}{2}(1+x^2), \quad (11)$$

$$d_F^{(2)}(x,Q^2) = \frac{1}{4}\frac{\beta}{2}\left[-\frac{1}{2}(1+3x^2)\ln x-(1-x)^2\right], \quad (12)$$

$$d_F^{(3)}(x,Q^2) = \frac{1}{8}\left(\frac{\beta}{2}\right)^2\left[(1-x)^2+\frac{1}{2}(3x^2-4x+1)\ln x + \frac{1}{12}(1+7x^2)\ln^2 x+(1-x^2)\mathrm{Li}_2(1-x)\right], \quad (13)$$

where $\beta = \frac{2\alpha}{\pi}(L-1), L = \ln(Q^2/m_e^2)$. Here α is the fine structure constant, m_e is the electron mass, Γ is the Gamma function, γ_E is Euler-Mascheroni constant. The integrations in (8) are taken over $\epsilon \le x_1, x_2 \le 1-\epsilon$ with $\epsilon = 10^{-6}$ for example.

III. NUMERICAL RESULTS

Our input parameters for the calculation are as follows. The fine structure constant in the Thomson limit is $\alpha^{-1}(Q^2 \to 0) = 137.0359895$. The mass of the Higgs boson is $M_H = 125$ GeV. Vectors weak boson masses are $M_W = 80.379$ GeV and $M_Z = 91.176$ GeV. For the lepton masses we take $m_e = 0.51099891$ MeV, $m_\mu = 105.658367$ MeV and $m_\tau = 1776.82$ MeV. For the quark masses, we take $m_u = 2.2$ MeV, $m_d = 4.7$ MeV, $m_c = 1.257$ GeV, $m_s = 95$ MeV, $m_t = 173$ GeV, and $m_b = 4.18$ GeV. We use $\lambda = 10^{-21}$ GeV, $C_{UV} = 0$, $k_c = 10^{-3}$ GeV, and $(\tilde{\alpha}, \tilde{\beta}, \tilde{\delta}, \tilde{\varepsilon}, \tilde{\kappa}) = (0,0,0,0,0)$ hereafter.

We defined percentate of full electroweak radiative corrections (and ISR corrections) as follows:

$$\delta_{\mathrm{EW/ISR}}[\%] = \frac{\sigma^{e^-e^+\to W^-W^+}_{\mathcal{O}(\alpha)/\mathrm{ISR}} - \sigma^{e^-e^+\to W^-W^+}_{\mathrm{T}}}{\sigma^{e^-e^+\to W^-W^+}_{\mathrm{T}}} \times 100\%. \quad (14)$$

In Fig. 2, the cross-sections (left panel for the case of $LR \equiv e_L^- e_R^+$ and right panel for the case of $RL \equiv e_R^- e_L^+$) and the corrections are presented as a function of the center-of-mass energy $\sqrt{s}$. The $\sqrt{s}$ are varied from 190 GeV to 1000 GeV. At the threshold of W-pair production ($\sqrt{s} \sim$ 200 GeV), we find that the cross-section is largest. It will be decreased beyond the peak. We find that $\sigma_{LR} > 10^2 \times \sigma_{RL}$. It is understandable that the dominant contributions from t-channel diagrams with exchanging ν_e only appear in LR case. In the below Figures, the full electroweak corrections (ISR corrections) for LR case change from -3% ($\sim -20\%$) to 14% ($\sim -10\%$), while the corresponding corrections for RL case vary from $\sim 5\%$ ($\sim -20\%$) to $\sim 50\%$ ($\sim -10\%$). The weak corrections are large contributions at higher-energy regions (they are $\sim 25\%$ for LR and $\sim 60\%$ for RL). It is well-known that the weak corrections in the high-energy region are attributed to the enhancement contribution of the single Sudakov logarithm [15]. It is clear that these corrections make a significant contributions and they must be taken into account at future lepton colliders.

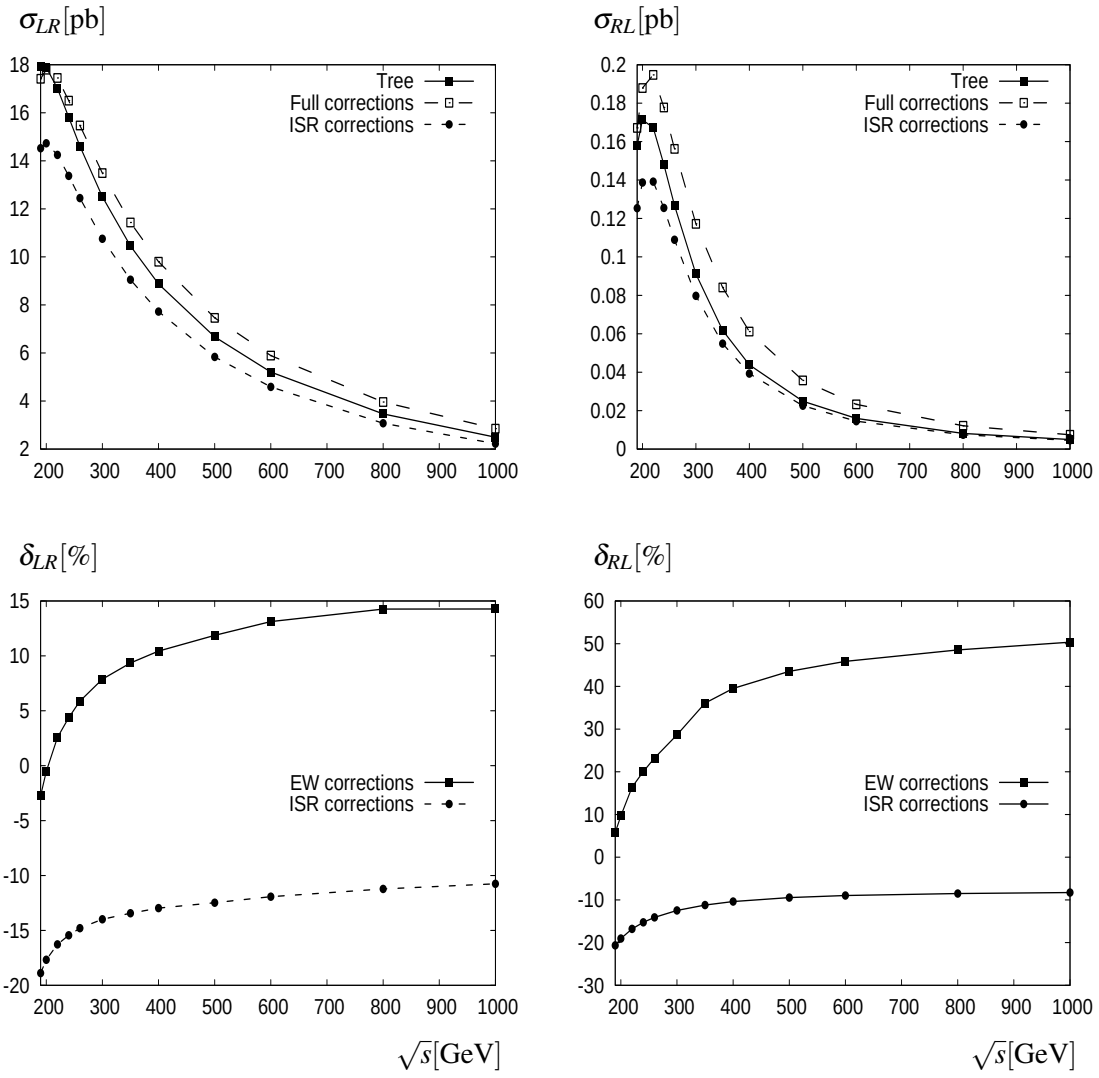

Fig. 2. The cross sections and corrections as a function of center-of-mass energy.

Because of the dominant contributions of *LR* in comparison with *RL* case, we only present in this article the distributions for *LR* case as examples. One of the most experimental interests is to the differential cross sections with respect to the transverse momentum of W^-. This distribution provides a useful information for the correctness of missing energy due to the decay of W-boson to neutrinos. Therefore, we can evaluate precisely the SM backgrounds in searching for new physics. The distribution at $\sqrt{s} = 500$ GeV is shown in Fig. 3. Here, we find that the ISR corrections are about -15% while full one-loop electroweak corrections are vary from 20% to -10% over the region. For the transverse momentum distribution, the cross sections are large around $P_{T,W^-} =$ 20 GeV. It is corresponding to the threshold of W-pair production. Both electroweak and ISR corrections are massive contributions. They must be taken into account at future lepton colliders.

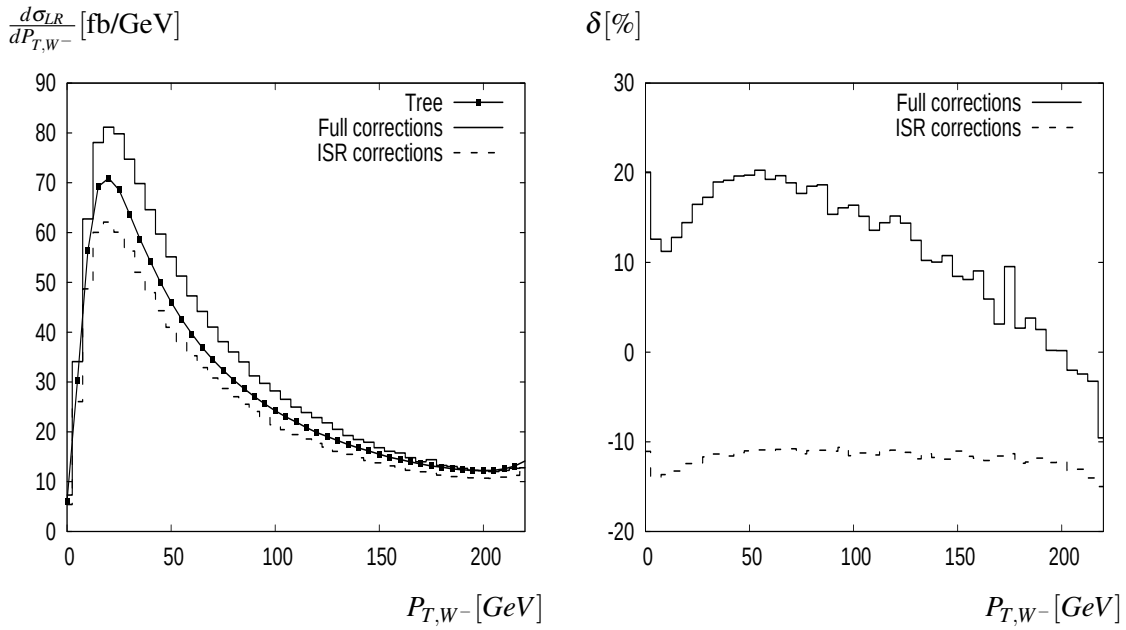

Fig. 3. Differential cross sections as a function of P_{T,W^-} at $\sqrt{s} = 500$ GeV.

IV. CONCLUSIONS

In this article, full $\mathcal{O}(\alpha)$ electroweak radiative corrections and $\mathcal{O}(\alpha^3)$ ISR corrections to the process $e^-e^+ \to W^-W^+$ with initial beam polarization effects at lepton colliders have been computed successfully. The corrections are order of 10% contributions to the cross sections as well as their relevant distributions. The corrections are massive contributions and they must be taken into account at future lepton colliders.

ACKNOWLEDGMENT

This research is funded by Vietnam National Foundation for Science and Technology Development (NAFOSTED) under grant number 103.01-2019.346.

REFERENCES

[1] H. Baer *et al.*, arXiv:1306.6352.
[2] M. Bohm, A. Denner, T. Sack, W. Beenakker, F. A. Berends and H. Kuijf, Nucl. Phys. B **304** (1988) 463.
[3] J. Fleischer, F. Jegerlehner and M. Zralek, Z. Phys. C **42** (1989) 409.
[4] W. Beenakker and A. Denner, Int. J. Mod. Phys. A **9** (1994) 4837.
[5] A. Denner, S. Dittmaier, M. Roth and D. Wackeroth, Phys. Lett. B **475** (2000) 127.
[6] A. Denner, S. Dittmaier, M. Roth and D. Wackeroth, Nucl. Phys. B **587** (2000) 67.
[7] J. H. Kühn, F. Metzler and A. A. Penin, Nucl. Phys. B **795** (2008) 277.
[8] M. Skrzypek and S. Jadach, Z. Phys. C **49** (1991) 577.
[9] M. Cacciari, A. Deandrea, G. Montagna and O. Nicrosini, Europhys. Lett. **17** (1992) 123.
[10] G. Belanger, F. Boudjema, J. Fujimoto, T. Ishikawa, T. Kaneko, K. Kato and Y. Shimizu, Phys. Rept. **430** (2006) 117.

[11] Z. Hioki, Acta Phys. Polon. B **27** (1996) 2573 [hep-ph/9510269].
[12] J. Fujimoto, M. Igarashi, N. Nakazawa, Y. Shimizu and K. Tobimatsu, *Suppl. Prog. Theor. Phys.* **100** (1990) 1.
[13] N. M. U. Quach, Y. Kurihara, K. H. Phan and T. Ueda, Eur. Phys. J. C **78** (2018) 422.
[14] G. Moortgat-Pick *et al.*, Phys. Rept. **460** (2008) 131 [hep-ph/0507011].
[15] M. Melles, Phys. Rept. **375** (2003) 219.

APPENDIX

For numerical checks, all the processes generated by GRACE-Loop are checked numerically. We show here the numerical checks for $e_L^- e_R^+ \to W^-W^+$ as a typical example.

Table 2. Test of C_{UV} independence of the amplitude. In this table, we take the nonlinear gauge parameters to be $(0,0,0,0,0)$, $\lambda = 10^{-21}$ GeV, $k_c = 10^{-3}$ and we use 500 GeV for the center-of-mass energy.

C_{UV}	$2\mathscr{R}e(\mathscr{M}_T^*\mathscr{M}_L)$ + soft contribution
0	-0.62719756935514104
10	-0.62719756935309612
100	-0.62719756933469639

Table 3. Test of the IR finiteness of the amplitude. In this table we take the nonlinear gauge parameters to be $(0,0,0,0,0)$, $C_{UV} = 0$, $k_c = 10^{-3}$ and the center-of-mass energy is 500 GeV.

λ[GeV]	$2\mathscr{R}e(\mathscr{M}_T^*\mathscr{M}_L)$ + soft contribution
10^{-20}	-0.62719756940107696
10^{-21}	-0.62719756935514104
10^{-22}	-0.62719756930912773

Table 4. Gauge invariance of the amplitude. In this table, we take $C_{UV} = 0$, $\lambda = 10^{-21}$ GeV, $k_c = 10^{-3}$ and we use 500 GeV for the center-of-mass energy.

$(\tilde{\alpha},\tilde{\beta},\tilde{\delta},\tilde{\varepsilon},\tilde{\kappa})$	$2\mathscr{R}e(\mathscr{M}_T^*\mathscr{M}_L)$ + soft contribution
$(0,0,0,0,0)$	-0.62719756935514104
$(1,2,3,4,5)$	-0.62719756947830896
$(10,20,30,40,50)$	-0.62719757052088487

Table 5. Test of the k_c-stability of the result. We choose the photon mass to be 10^{-21} GeV and the center-of-mass energy is 500 GeV. The second column presents for the sum of virtual one-loop and soft photon cross-sections and the third column shows for the hard photon cross-section. The last column is the sum of both.

k_c [GeV]	σ_{T+L+S} [pb]	σ_H [pb]	σ_{total} [pb]
10^{-5}	-5.079 ± 0.002	12.529 ± 0.006	$7.45(1)$
10^{-4}	-3.374 ± 0.001	10.821 ± 0.005	$7.44(7)$
10^{-3}	-1.669 ± 0.001	9.119 ± 0.004	$7.45(0)$
10^{-2}	0.0353 ± 0.0004	7.414 ± 0.003	$7.44(9)$